JAERI-M
9472

# BALLOONING STABLE HIGH BETA TOKAMAK EQUILIBRIA

April 1981

Takashi TUDA, Masafumi AZUMI, Gen-ichi KURITA
Tomonori TAKIZUKA and Tatsuoki TAKEDA

日本原子力研究所
Japan Atomic Energy Research Institute

# Ballooning Stable High Beta Tokamak Equilibria

Takashi TUDA, Masafumi AZUMI, Gen-ichi KURITA, Tomonori TAKIZUKA and Tatsuoki TAKEDA

Division of Thermonuclear Fusion Research, Tokai Research Establishment, JAERI

(Received April 9, 1981)

The second stable regime of ballooning modes is numerically studied by using the two-dimensional tokamak transport code with the ballooning stability code. Using the simple FCT heating scheme, we find that the plasma can locally enter this second stable regime. And we obtained equilibria with fairly high beta ($\beta \sim 23\%$) stable against ballooning modes in a whole plasma region, by taking into account of finite thermal diffusion due to unstable ballooning modes. These results show that a tokamak fusion reactor can operate in a high beta state, which is economically favourable.

Keywords; Ballooning Mode Instability, Second Stable Region, High Beta Tokamak Equilibrium, Two-Dimensional Tokamak Code, Numerical Solution, Finite Thermal Diffusion

JAERI-M 9472

# バルーニング・モードに対して安全な高ベータ・トカマク平衡

日本原子力研究所東海研究所核融合研究部
津田　　孝・安積　正史・栗田　源一
滝塚　知典・竹田　辰興

（1981年4月9日受理）

2次元トカマク・コードとバルーニング・モード不安定性解析コードを組合せることにより，バルーニング・モードの第2安定領域の平衡について数値的に解析した。単純なFCT（磁束保存型）加熱過程を用いて加熱を行うことによって，局所的に第2安定領域に入っているプラズマ平衡を作ることができる。このように局所的に第2安定領域にあるプラズマについて，バルーニング不安定性に基く熱拡散を考慮にいれることにより全プラズマ領域でバルーニング・モードに対して安定な，かなり高いベータ値（$\beta\sim 23\%$）を持つ安定平衡を得ることができる。この結果は，トカマク型核融合炉を，経済的に有利な高ベータ状態で運転し得ることを示している。

目次なし

The economics of a tokamak fusion reactor will be considerably improved by the operation in a high beta state, where beta $\beta$ is the ratio of the plasma pressure to the magnetic pressure. Although the concept of a flux-conserving tokamak (FCT) [1] removes the limitation of the beta value from the viewpoint of the MHD equilibrium, MHD instabilities may restict the possible beta value in a tokamak. Among these instabilities, ballooning modes have been considered the most restrictive ones. The simple estimation by neglecting the effect of the shear gives the critical beta value against these modes as $\beta_c \sim 1/q^2 A$, where q is the safety factor and A is the aspect ratio. The ballooning modes in a tokamak with finite shear were first analysed by Connor, Hastie and Taylor [2], and the improvement in the critical beta value by the change of the plasma shape and the current profile has been studied by many authors [3 -6]. When the plasma is heated up beyond this critical value and the beta exceeds the second critical value, Coppi et al. found analytically that ballooning modes can be stabilized again [7]. Strauss et al.[8] studied this second stable regime of ballooning modes numerically by the use of the reduced set of MHD equations, in which the terms of order of $A^{-2}$ and $\beta^2$ are neglected. The contribution of these terms, however, is essential to the second stability regime of ballooning modes. The purpose of this papar is to show fairly high beta tokamak equilibria, which are stable against ballooning modes over the whole plasma region, by using the two-dimensional tokamak transport equations and the ballooning mode equation described in Ref.[2].

The basic equations are the combination of the surface averaged transport equations of simplified FCT version

$$\frac{\partial}{\partial t} p\left(\frac{\partial V}{\partial \psi}\right)^{5/3} = \left(\frac{\partial V}{\partial \psi}\right)^{3/2} \frac{\partial}{\partial \psi}\left(\chi_p \frac{\partial V}{\partial \psi}\frac{\partial p}{\partial \psi}\right) + S(\psi)\left(\frac{\partial V}{\partial \psi}\right)^{5/3} \tag{1}$$

$$\frac{\partial}{\partial t} q = 0 \quad , \tag{2}$$

and the axisymmetric toroidal MHD equilibrium equation

$$R\frac{\partial}{\partial R}\left(\frac{1}{R}\frac{\partial \psi}{\partial R}\right) + \frac{\partial^2 \psi}{\partial Z^2} = -R^2 \frac{dp}{d\psi} - T\frac{dT}{d\psi} \tag{3}$$

where $\psi$, V, p, S, and T are the poloidal magnetic flux, the volume surrounded by a contour of $\psi$, the plasma pressure, the pressure source, and the poloidal current flux, respectively. In order to manifest the effect of unstable ballooning modes on the plasma transport, only the anomalous thermal conductivity $\chi_p$ due to these instabilities is taken into account and the electric conductivity is assumed infinitely large. We start the computation from the force-free equilibrium with the toroidal current density $j_\phi$

$$R j_\phi = \alpha_0 \{ 1 - \alpha_1 \psi - (1 - \alpha_1) \psi^4 \} \quad , \tag{4}$$

where $\psi$ is normalized such that $\psi$=0 at the magnetic axis and $\psi$=1 at the plasma surface. Parameters $\alpha_0$ and $\alpha_1$ are adjusted such that the values of the safety factor at the magnetic axis $q_a$ and at the surface $q_s$ take the prescribed ones. Figure 1 shows the force-free equilibrium with circular cross section, A=3, $q_a$=1 and $q_s$=3. Now this force-free plasma is heated to higher beta by the pressure source $S(\psi)=(1-\psi^2)^2$. As was reported in Ref.[6], the beta value saturates at $\beta$=2.8%, when the thermal conductivity becomes infinitely large on magnetic surfaces unstable against ballooning modes. In order to study the second stable regime, in this work, we set $\chi_p$=0 during the heating process, which means the plasma is heated up much faster than the diffusion time scale. When $\beta$ becomes about 2%, the unstable region appears in a plasma and this region spreads towards both the magnetic axis and the plasma boundary with increasing $\beta$. When the plsma pressure is further increased, however, the growth rate around the magnetic surface $\psi$=0.6 begins to decrease at $\beta \sim 6\%$, and the second stable region appears in the midway of the unstable region when $\beta$ exceeds 10%, as was predicted by Coppi et al. [7]. The shaded region in Fig. 2 corresponds to the unstable region in the $\psi$-$\beta$ plane, and the second stable region is well shown. Equilibria with $\beta$=13% and $\beta$=34% are shown in Fig. 3 and Fig. 4, respectively, where $dp/d\psi|_{crit}$ is the critical pressure gradient, above which ballooning modes become unstable (Appendix). It must be noted that local interchange modes are always stable during this sequence. In this way, the plasma locally enter the second stable regime, but unfortunately, this simple heating scheme with constant source profile can not achieve the equilibrium stable over the whole plasma region. Now, we turn off the pressure source and take into account of the finite thermal conductivity due to unstable ballooning modes. The themal diffusion reduces the pressure gradient on unstable magnetic surfaces and increases it on neighboring stable surfaces, so that the unstable region spreads toward the stable region with decreasing the difference between $dp/d\psi$ and $dp/d\psi|_{crit}$. Therefore, if the second stable region has the enough margin to absorb the contribution of the initially unstable region, then the plasma can reach the stable state over the whole region. Figures 5 and 6 show the ballooning stable equilibria with $\beta = 12\%$ and $\beta = 23\%$, respectively. These equilibria were achieved from the equilibria with $\beta = 13\%$ (Fig. 3) and $\beta = 34\%$ (Fig. 4), respectively. It is worth to note that these high beta equilibria still have the margin of the difference between $dp/d\psi$ and $dp/d\psi|_{crit}$; this means that it is possible to obtain ballooning stable equilibria with much higher beta values.

Our scheme to achieve the ballooning stable high beta equilibrium is summarized as follows: The plasma is heated up by the pressure source with the constant profile much faster than the dissipation due to unstable ballooning modes. When the plasma locally enters the second stable regime, we turn off the heating. Then the plasma relaxes to the ballooning stable state by the thermal diffusion due to unstable modes. Finally, the fairly high beta plasma stable over the whole region can be achieved. The possibility to realize the plasma with locally second regime, however, is dependent on the maximum growth rate, the difference between the first and second critical beta values, and the ratio of the heating time to the anomalous diffusion time. First two problems may be solved by optimizing plasma parameters, especially q-profile, and by taking into account of kinetic effects including the pressure anisotropy, while the last problem remains as the important theoretical work in future.

The authors would like to thank the members of Plasma Theory Laboratory for their fruitful discussions. It is a great pleasure to acknowledge helpful discussion and continuing encouragement of Dr. M. Tanaka. We would also like to express our sincere thanks to Dr. Y. Obata for his encouragement throughout the whole work.

References

[1] J.F. Clarke and D.J. Sigmar, Phys. Rev. Lett. 38 (1977) 70.

[2] J.W. Connor, R.T. Hastie and J.B. Taylor, Proc. Roy. Soc. A365 (1971) 1.

[3] A.M.M. Todd et al., Nucl. Fusion 19 (1979) 743.

[4] R.A. Dory et al., Plasma Physics and Controlled Nuclear Fusion Research 1978 (Proc. 7th International Conf. Innsbruck, 1978), Vol.1, IAEA, Vienna 1979, p.579.

[5] D. Dobrott et al., ibid p.731.

[6] M. Azumi et al., Plasma Physics and Controlled Nuclear Fusion Research Brussels, 1980, IAEA-CN-38/K-1-1 in press.

[7] B. Coppi et al., Nucl. Fusion 16 (1979) 715.

[8] H.R. Strauss et al., Nucl. Fusion 20 (1980) 638.

Appendix Critical pressure gradient

The critical pressure gradient $dp/d\psi|_{crit}$ against the infinitely high-n ballooning mode on a magnetic surface is obtained from the ballooning mode equation described in Ref. [2] with the zero growth rate;

$$\frac{d}{ds}\left(f\frac{d\phi}{ds}\right)+\left(\frac{dp}{d\psi}\right)_{crit} g\,\phi = 0$$

$$f = \frac{1}{R^2 B_p}\left[1+\left(\frac{R^2 B_p^2}{B} z\right)^2\right]$$

$$g = \frac{1}{R^2 B_p}\left[\frac{\partial}{\partial\psi}(2p+B^2) - \frac{RB_t B_p}{B} z \frac{\partial B^2}{\partial s}\right]$$

$$z = \int_0^s \frac{ds}{JB_p}\frac{\partial}{\partial\psi}\left(\frac{JB_t}{R}\right)$$

where s is the arc length and J is Jacobian. This equation is solved as the eigenvalue problem by using the finite element method;

$$(A - \lambda B)\phi = 0 .$$

The tridiagonal matrices A and B take the form

$$A_{i,i+1} = A_{i+1,i} = \frac{f_{i+1/2}}{(\Delta s)^2}$$

$$A_{i,i} = -\frac{f_{i+1/2}+f_{i-1/2}}{(\Delta s)^2}$$

$$B_{i,i+1} = B_{i+1,i} = -g_{i+1/2}$$

$$B_{i,i} = -(g_{i+1/2} + g_{i-1/2}) ,$$

where the subscript i represents the mesh number in the s direction. The largest eigenvalue $\lambda$, which is obtained by the bisectional method, corresponds to the critical pressure gradient $dp/d\psi|_{crit}$.

Figure Captions

Fig. 1 Force-free equilibrium with $A = 3.0$, $q_a = 1$ and $q_s = 3$. The current profile is chosen as Eq.(4).
(a) $\sqrt{\psi}$ contours for $0 \leq \psi \leq 1$. (b) Profiles of the surface averaged current density J, the safety factor Q , and the shear S as functions of $\psi$. (c) Profiles of the current density and the pressure as functions of R on the midplane Z=0. (d) Profiles of the pressure P, the pressure gradient $\frac{dp}{d\psi}$ (DP) and the critical pressuregradient $\frac{dp}{d\psi}\big|_{crit}$ (DP-C) as functions of $\psi$. The region of $\frac{dp}{d\psi} > \frac{dp}{d\psi}\big|_{crit}$ is unstable against ballooning modes.

Fig. 2 Ballooning unstable region in the $\psi - \beta$ plane of the plasma, which is heatedup with pressure source $S(\psi) = (1 - \psi^2)^2$ from the force-free equilibrium shown in Fig. 1.

Fig. 3 FCT equilibrium with $\beta = 13\%$.

Fig. 4 FCT equilibrium with $\beta = 34\%$.

Fig. 5 Equilibrium with $\beta = 12\%$ stable against ballooning modes in a whole plasma region.

Fig. 6 Equilibrium with $\beta = 23\%$ stable against ballooning modes in a whole plasma region.

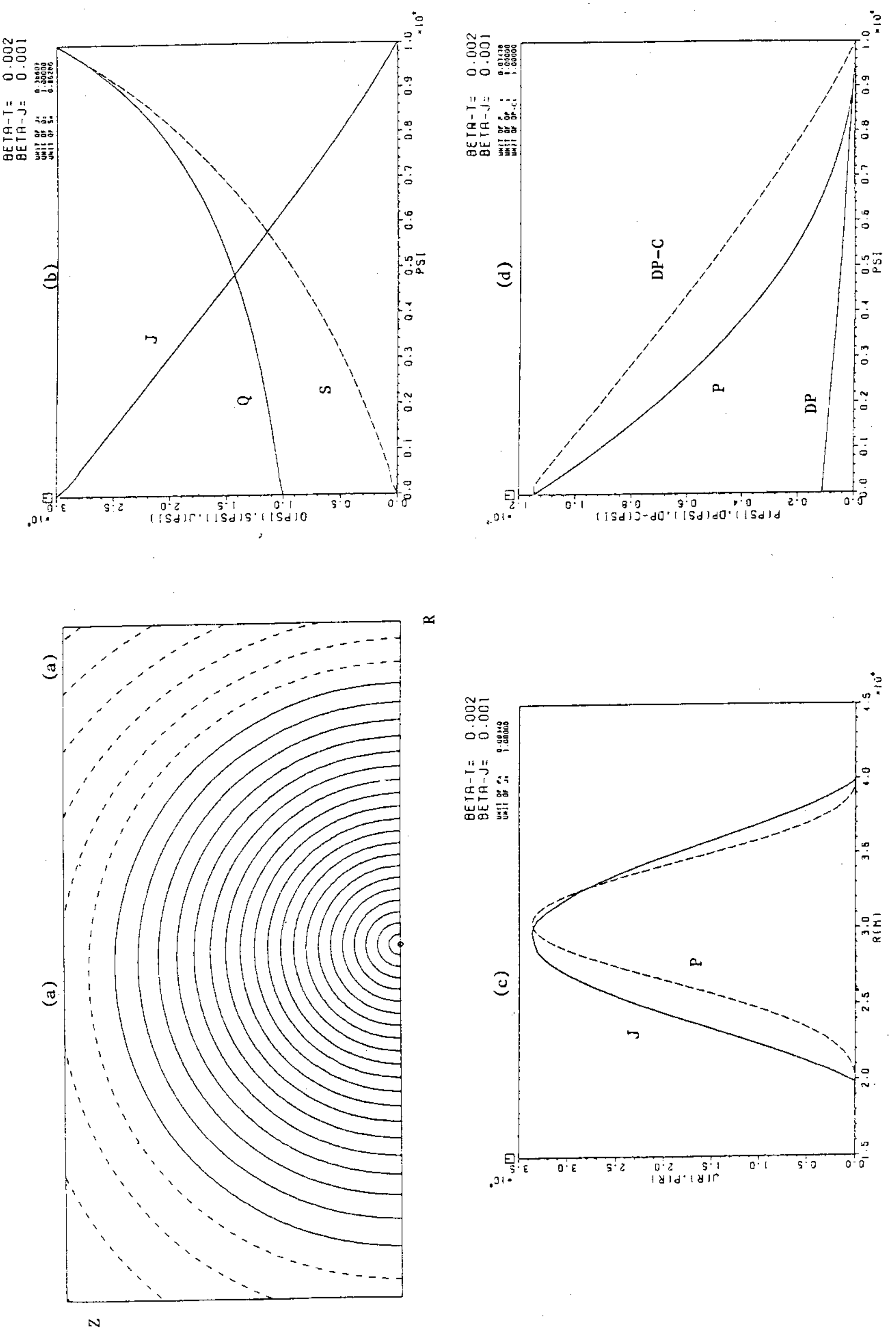
(a)
R
Z
(b)
BETA-T= 0.002
BETA-J= 0.001
J
Q
S
PSI
Q(PSI),S(PSI),J(PSI)
(c)
BETA-T= 0.002
BETA-J= 0.001
J
P
R(M)
J(R),P(R)
(d)
BETA-T= 0.002
BETA-J= 0.001
DP-C
P
DP
PSI
P(PSI),DP(PSI),DP-C(PSI)

Fig. 1

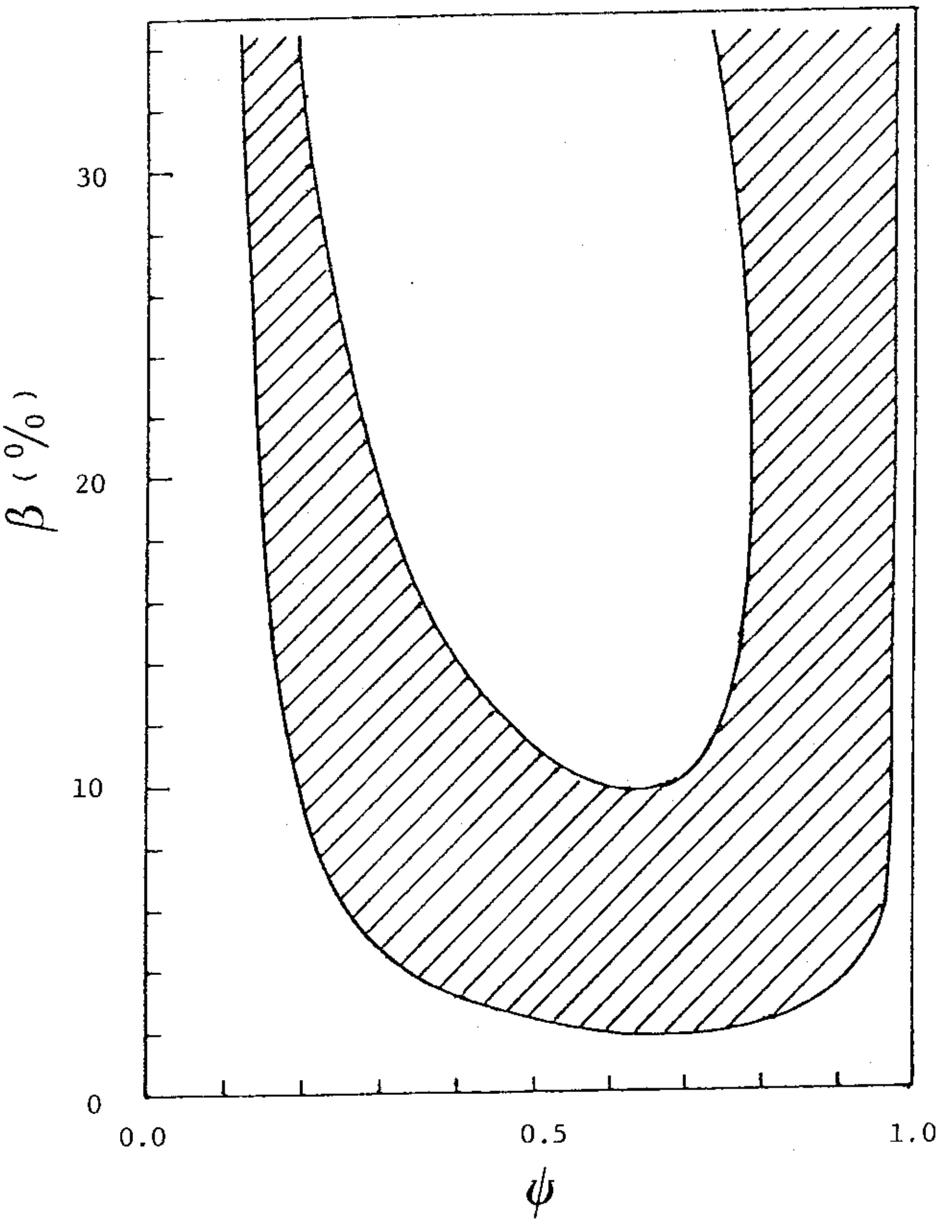


Fig. 2

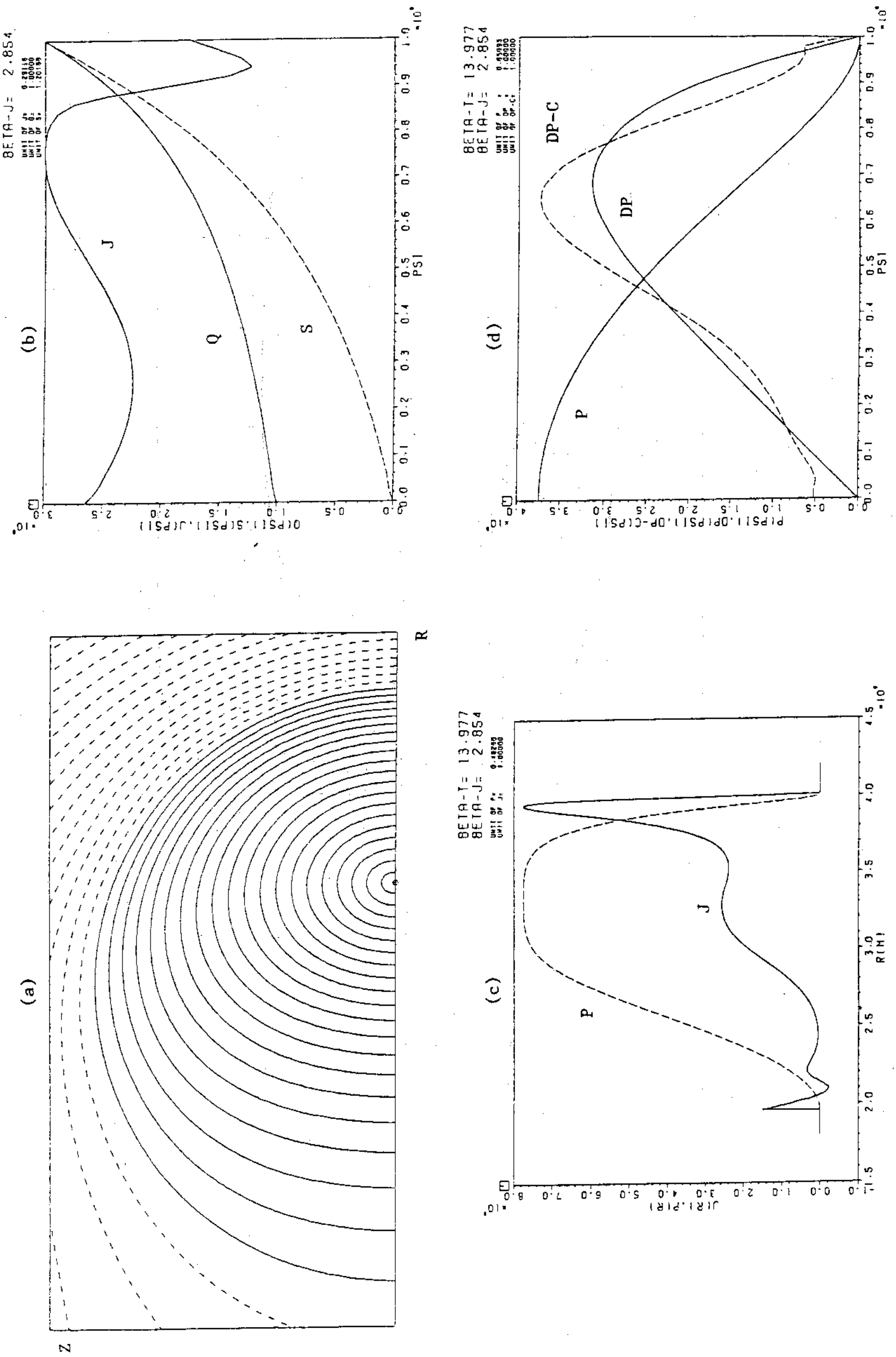
(a)
Z
R
(b)
BETA-T= 13.977
BETA-J= 2.854
J
Q
S
PSI
Q(PSI),S(PSI),J(PSI)
(c)
BETA-T= 13.977
BETA-J= 2.854
P
J
R(M)
J(R),P(R)
(d)
BETA-T= 13.977
BETA-J= 2.854
DP-C
DP
P
PSI
P(PSI),DP(PSI),DP-C(PSI)

Fig. 3

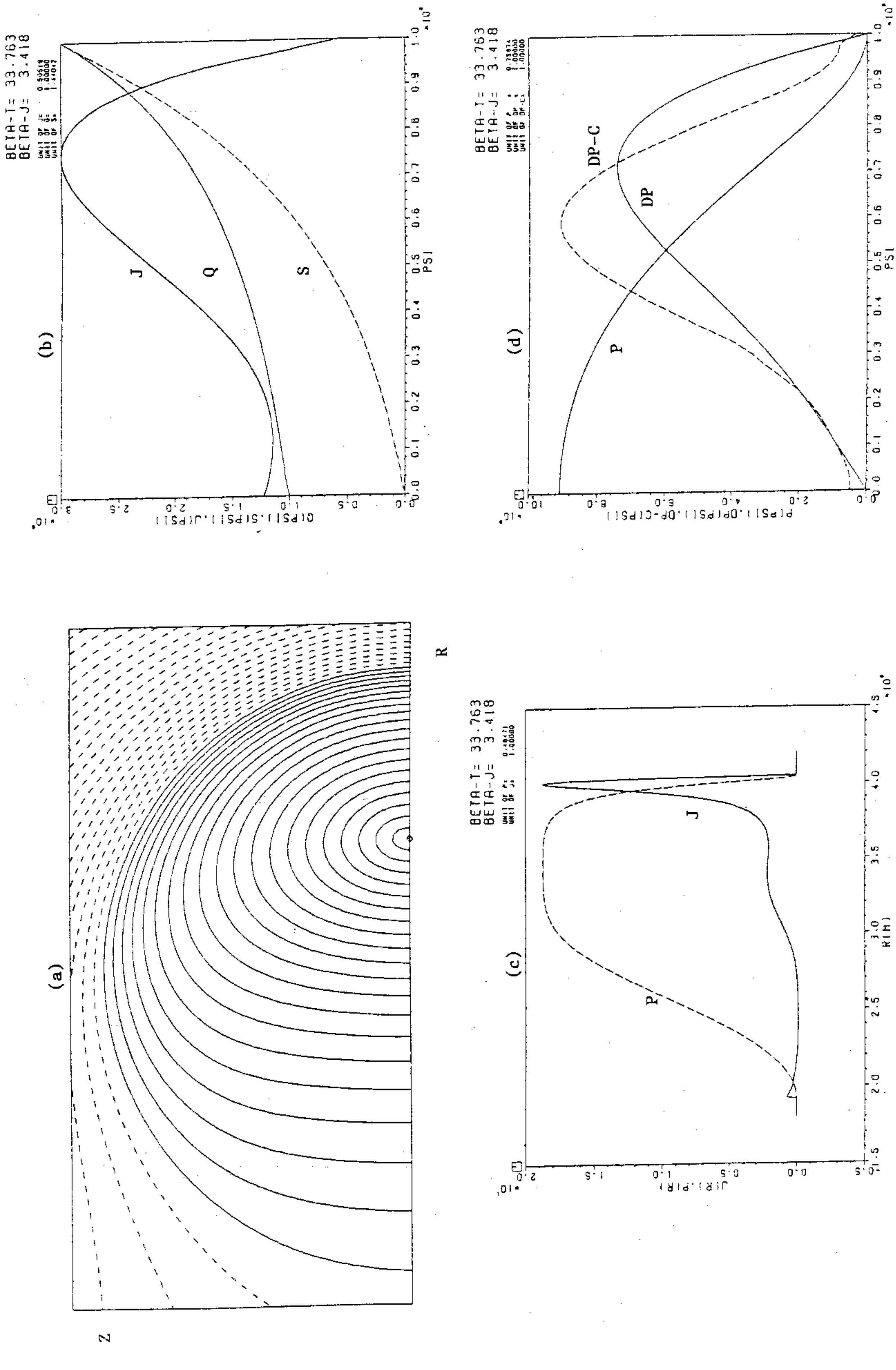
(a)
R
Z
(b)
BETA-T= 33.763
BETA-J= 3.418
J
Q
S
PSI
(c)
BETA-T= 33.763
BETA-J= 3.418
P
J
R(M)
(d)
BETA-T= 33.763
BETA-J= 3.418
DP-C
DP
P
PSI

Fig. 4

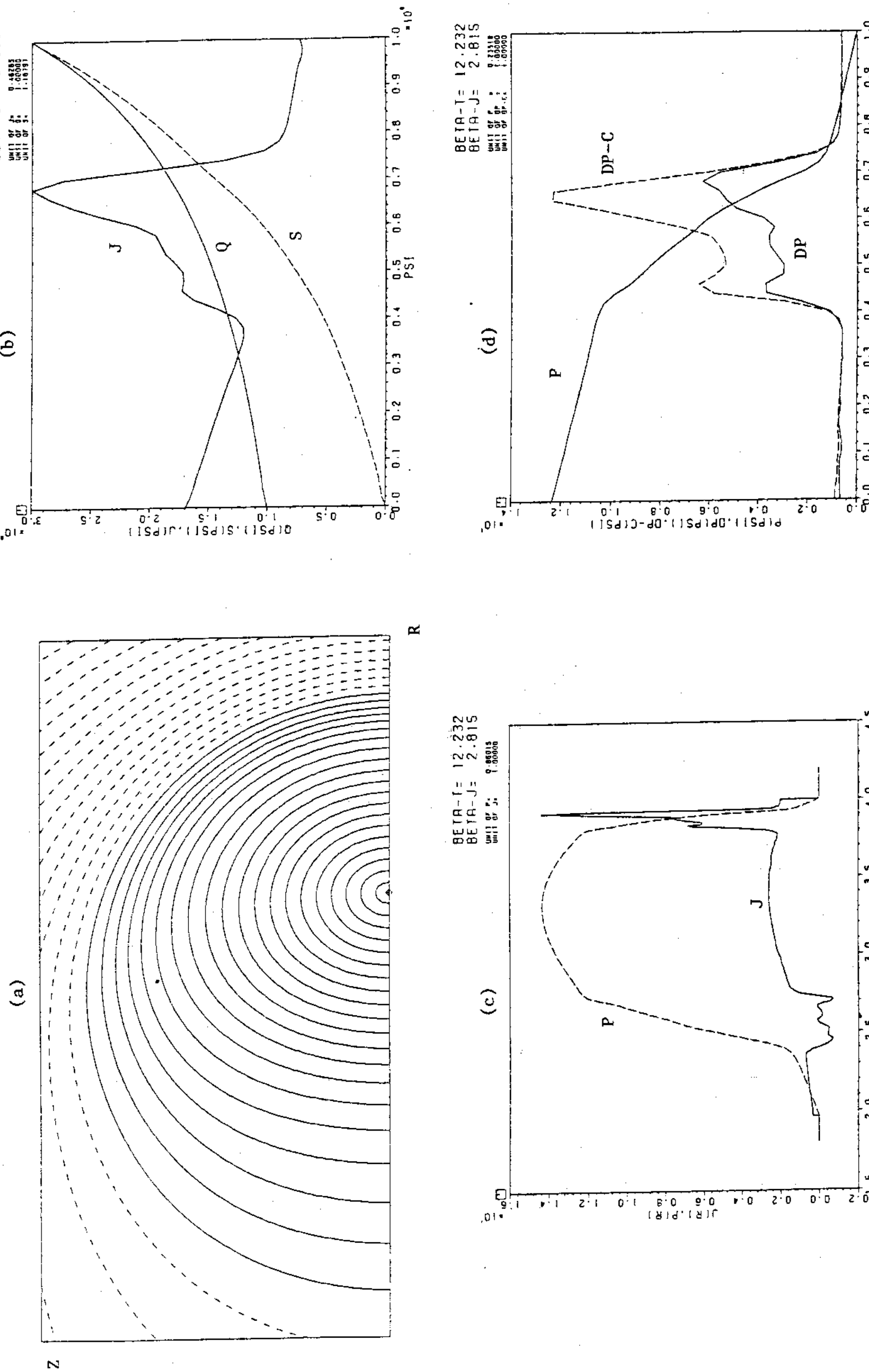
(a)
R
Z
(b)
BETA-T= 12.232
BETA-J= 2.815
J
Q
S
PSI
Q(PSI),S(PSI),J(PSI)
(c)
BETA-T= 12.232
BETA-J= 2.815
P
J
R(M)
J(R),P(R)
(d)
BETA-T= 12.232
BETA-J= 2.815
P
DP
DP-C
PSI
P(PSI),DP(PSI),DP-C(PSI)

Fig. 5

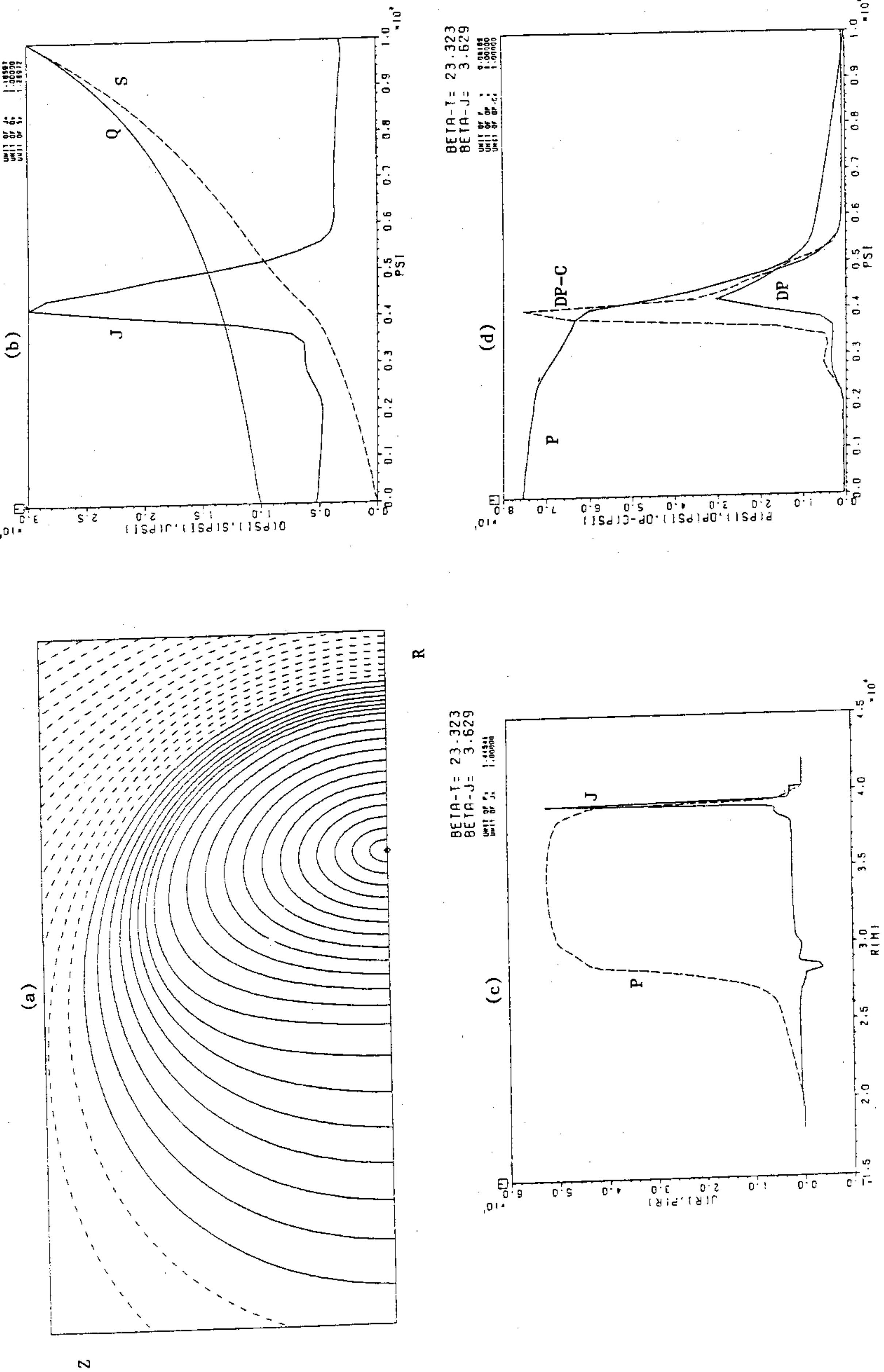


Fig. 6